GONG Catalog of Solar Filament Oscillations Near Solar Maximum

M. Luna[1,2], J. Karpen[3], J. L. Ballester[4,5], K. Muglach[3,6], J. Terradas[4,5], T. Kucera[3] and H. Gilbert[3]

[1] Instituto de Astrofísica de Canarias, E-38200 La Laguna, Tenerife, Spain
[2] Departamento de Astrofísica, Universidad de La Laguna, E-38206 La Laguna, Tenerife, Spain
[3] NASA Goddard Space Flight Center, Greenbelt, MD 20771, USA
[4] Departament de Física, Universitat de les Illes Balears (UIB), E-07122 Palma de Mallorca, Spain
[5] Institute of Applied Computing & Community Code (IAC^3), UIB, Spain
[6] Catholic University of America, Washington, DC 20064, US

BUKS2018, La Laguna, Tenerife, September 3-7 2018

Luna, Karpen, Ballester, Muglach, Terradas, Kucera & Gilbert (2018), The Astrophysical Journal Supplement Series, 236, id. 35

Recent observations

- Nowadays, thanks to both space- and ground-based instruments, observations of flare-induced oscillations have become common.
- Exciters: Moreton/EIT waves, nearby jets, flares, partial eruptions and the **internal processes during an eruption (no triggering agent observed)** (see **Luna et al. 2018** and **Arregui et al. 2018** for references).
- Many of the observed flare-induced oscillations exhibit motions in different polarization (relative to the filament axis): vertical, horizontal, longitudinal, or mixed character.
- Example 1, Example 2, Example 3.

One of the largest oscillation ever reported: **Luna et al. (2017), ApJ, 850, id. 143**

- Eruption of a filament segment produces velocities of up to 100 $\mathrm{km\,s^{-1}}$ in other segment.
- GONG Hα
- AIA 171Å

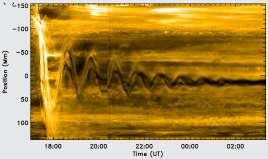

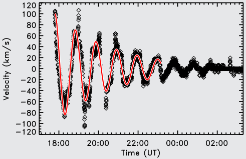

Motivation

Objective and plan

- Prove that LAOs are common and increase observational evidence.
- Global study of LAOs on the Sun using GONG Hα data during a solar cycle: in this first study we focus on the solar maximum.
- This study can shed light on the global evolution of prominences and solar activity, and help us understand the relation of prominence oscillations and eruptions.
- The scientific community will have available a survey of LAOs to perform in-depth analysis of events using SDO or STEREO.

Description of the catalog

- Survey from the GONG network Hα data during January - June 2014: solar maximum of cycle 24.
- Large variety of oscillations: strongly damped motions, undamped oscillations, and amplified oscillations.
- Statistically significant study of filament oscillations of this kind and their pertinent properties.
- Online catalog: `http://www.iac.es/galeria/mluna/pages/gong-catalogue-of-laos.php`.
- Use also the shortened version `http://goo.gl/VxkeiV`

Why GONG?

- Filaments and their oscillations detected easily with Hα GONG images.
- Global Oscillation Network Group (GONG; `http://gong2.nso.edu`): Learmonth (L), Udaipur (U), El Teide (T), Cerro Tololo (C), Big Bear (B) and Mauna Loa (M).
- The telescope locations were selected to follow the diurnal motion of the Sun in the sky, in order to collectively ensure full-day coverage.
- The temporal cadence of the GONG data is 1 min with a pixel size of $\sim$1 arcsec.

Event Selection

1. Detect the filaments that may oscillate by **visual inspection**: we identified 408 potential cases.
2. In-depth analysis downloading the data and constructing time-distance diagrams.
3. We check the time-distance diagrams and discard the events where a no clear oscillatory pattern is detected: 196 oscillations of the 408 initial potential candidates.

Triggering and Filament Parameters

- Triggering agents (43% cases): flares (FLARE), prominence eruption (PE), jets (JET), and Moreton Wave (MW, 1 case)

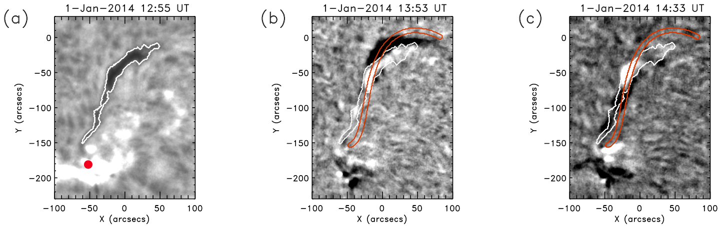

- Curved artificial slits to construct time-distance diagrams.
- We parametrize the filament (length and width).
- Direction of motion α is also measured.

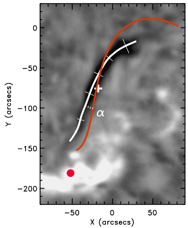

Time-distance diagrams and Oscillation analysis

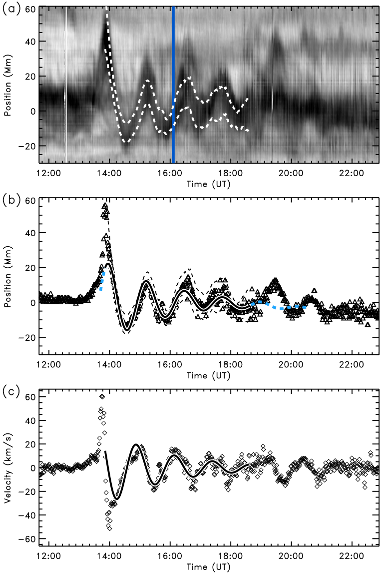

- The slit, of length *l* and width *w* pixels, was placed lengthwise along the curved path of the motion.
- We averaged the intensity over the transverse pixels, *w*, resulting in an intensity distribution along *l*.
- The central position of each filament on the time-distance diagram is computed by fitting a Gaussian function to the intensity as

$$I(s) = g_0\, e^{-\frac{1}{2}\left(\frac{s-s_0}{\sigma_{\mathrm{G}}}\right)^2} + g_2 + g_3\, s + g_4\, s^2$$

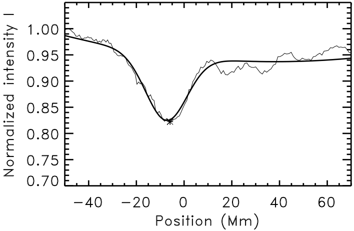

Time-distance diagrams and Oscillation analysis

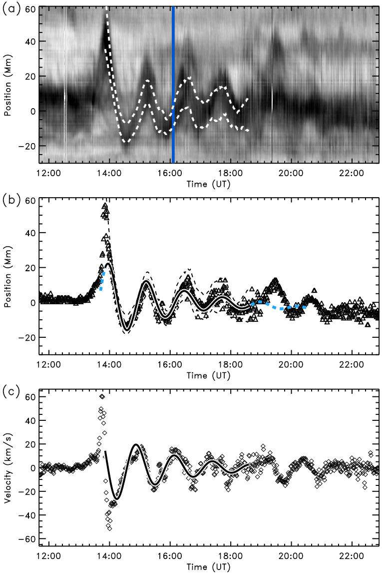

- We consider the error of the position as $\sigma = 0.5\,\sigma_{\rm G}$ (dashed line).
- We fit $s_0(t)$, as

$$
\begin{aligned}
y(t) \quad = \quad & A_0 e^{-A_1 (t-t_0)} \cos\left[A_2 (t - t_0) + A_3\right] + \\
& A_4 + A_5\,(t - t_0) + A_6\,(t - t_0)^2 + A_7\,(t - t_0)^3 \,.
\end{aligned}
$$

- The measured velocity is $\frac{ds_0(t)}{dt}$
- $\alpha = 16^\circ$, $P = 76 \pm 1$ min, $\tau = 121 \pm 15$ min, $A = 23 \pm 2$ Mm, $V = 26 \pm 4\ \mathrm{km\,s^{-1}}$ and $\tau/P = 1.6 \pm 0.2$.

Event 58: LALO triggered by a two-ribbon flare

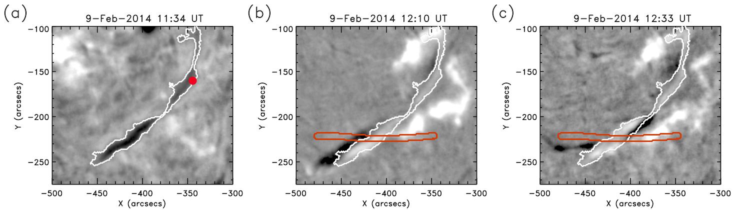

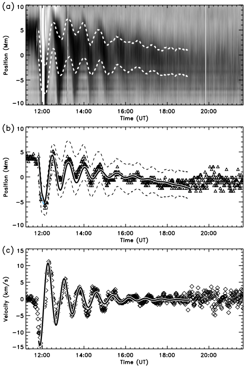

- LAO with a peak velocity of 14 $\mathrm{km\,s^{-1}}$, triggered by a two-ribbon flare that straddled the AR filament.
- $\alpha = 32°$, $P = 47 \pm 1$ min, $\tau = 82 \pm 20$ min, $\tau/P = 1.8 \pm 0.4$ $A = 5 \pm 2$ Mm

Event 63: LALO in a large quiescent filament

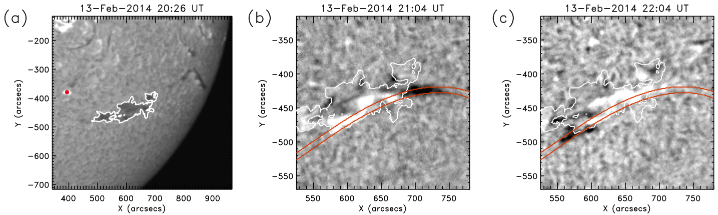

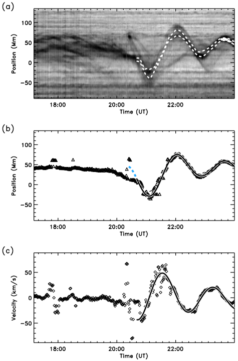

- LALO with a peak velocity of $48.5 \pm 2.4\,\mathrm{km\,s^{-1}}$, triggered by a closer flare.
- $\alpha = 2°$, $P = 103 \pm 1$ min, $\tau = 175 \pm 12$ min, $\tau/P = 1.7 \pm 0.1$, $A = 47 \pm 2$ Mm

Event 91: LALO triggered by a Moreton wave

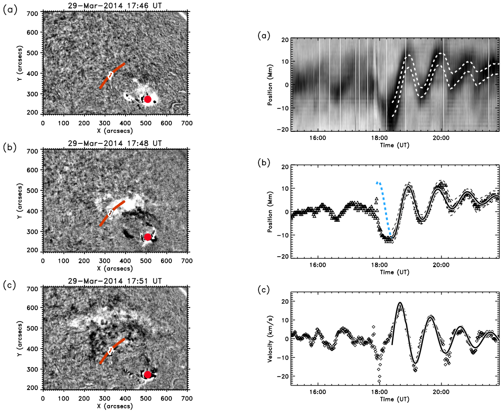

LALO with $V = 19.3 \pm 2.3\,\mathrm{km\,s^{-1}}$, a peak displacement $A = 11 \pm 1$ Mm, period $P = 58 \pm 1$ min, damping time $\tau = 108 \pm 12$ min, and $\tau/P = 1.9 \pm 0.2$. The angle between the motion and the filament spine was $\alpha = 26°$.

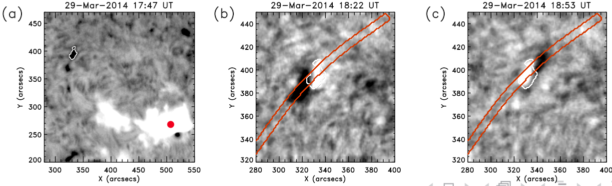

Event 107 and 108*: Double event with amplified oscillation and eruption

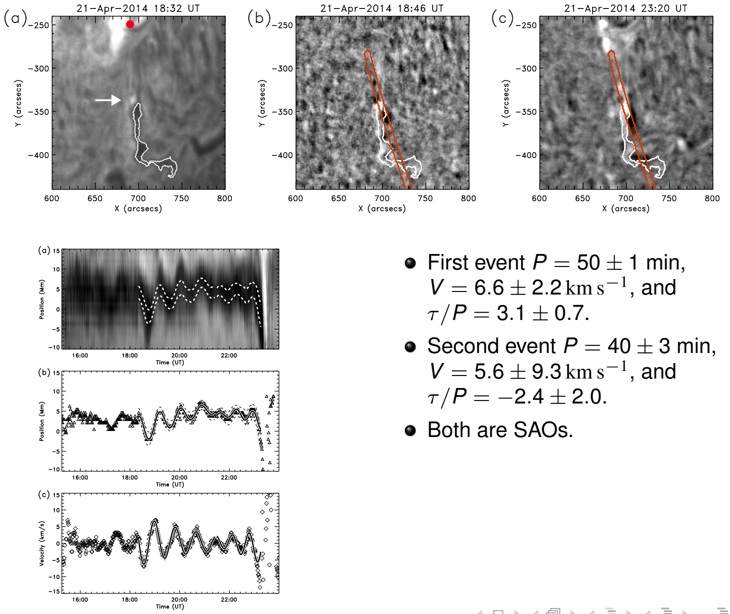

- First event $P = 50 \pm 1$ min, $V = 6.6 \pm 2.2\,\mathrm{km\,s^{-1}}$, and $\tau/P = 3.1 \pm 0.7$.
- Second event $P = 40 \pm 3$ min, $V = 5.6 \pm 9.3\,\mathrm{km\,s^{-1}}$, and $\tau/P = -2.4 \pm 2.0$.
- Both are SAOs.

Statistics:

- 196 oscillation events in 6 months near maximum of cycle 24.
- 43% trigger identified: 72 flares, 11 prominence eruptions, 1 jet, and 1 Moreton wave.
- In 111 cases the triggering agent was not identified.
- In 9 cases the filament erupted during the temporal range analyzed.
- We classified in SAOs ($V < 10\,\mathrm{km\,s^{-1}}$) and LAOs ($V > 10\,\mathrm{km\,s^{-1}}$).
- 196 oscillation events: 106 SAOs and 90 LAOs.
- **One oscillation event per day on the visible solar disk.**
- The occurrence rate of one LAO event every two days implies that **LAOs are a common phenomena on the** Sun, in contrast to previous statements that LAOs are scarce.
- Similar rate for SAOs.

Statistics

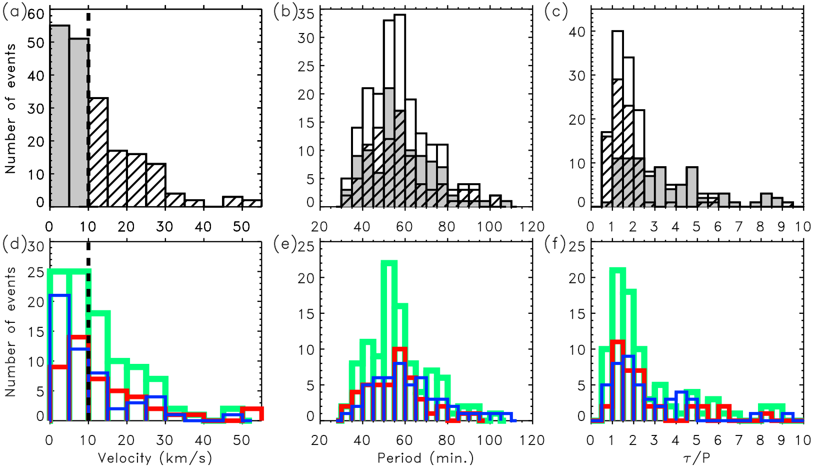

- No clear two populations in V distribution.
- **Clear peak centered at $\sim$58 min**.
- LAO events are mainly below $|\tau/P| = 3$ while SAOs cover a larger range.
- Similar results for all filament types.

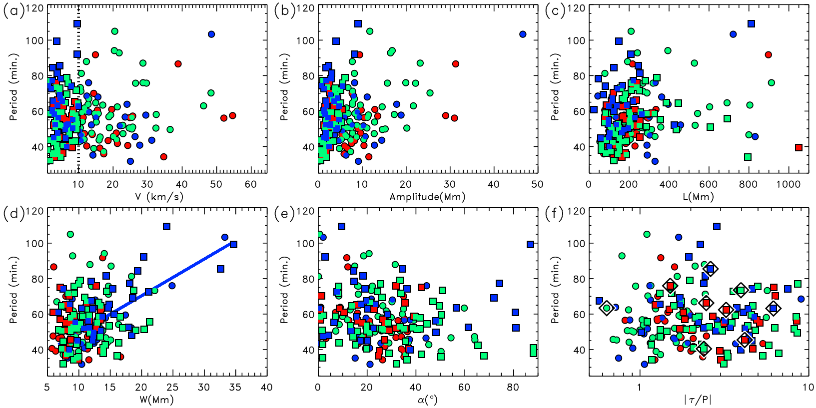

- No dependence of P with V, A, L, or τ
- Weak dependence with W in QS filaments. The general tendency is for wider QS filaments to oscillate with longer periods than narrower prominences.
- For angles $\alpha < 70^{\circ}$, the range of possible periods generally decreases with α.

GONG Catalog
Luna, Karpen, Ballester, Muglach, Terradas, Kucera and Gilbert

Introduction
Description of GONG catalog
Event Selection
Triggering
Oscillation analysis
Cases
Statistics
Seismology
Summary

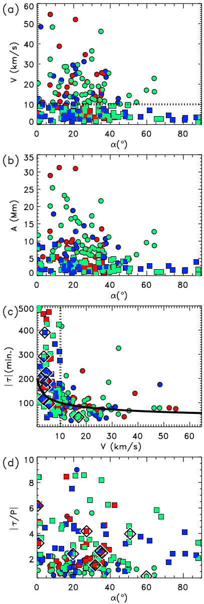

- The $V - \alpha$ scatter plot shows a clear pattern: the V range decreases with α, and the V values drop sharply for events with α beyond 40°.
- This tendency leads to no LAOs for $\alpha > 65^\circ$.
- The two populations can be also distinguished in the $A - \alpha$ scatter plot .
- This suggests some connection with the polarization of the oscillation.
- Larger velocity amplitudes are positively correlated with stronger damping, which indicates that the higher-speed oscillations are likely to be nonlinear.
- The scatter plot $|\tau/P|$ also decreases as V increases (not shown).
- **Zhang et al. (2013)** found a nonlinear relationship between τ and V in their simulations of prominence mass formation: $\tau \sim V^{-0.3}$.
- This scaling law (solid black line in (c)) is roughly consistent with observed and derived values from our events, suggesting LAOs may be damped through radiative cooling.

Statistics

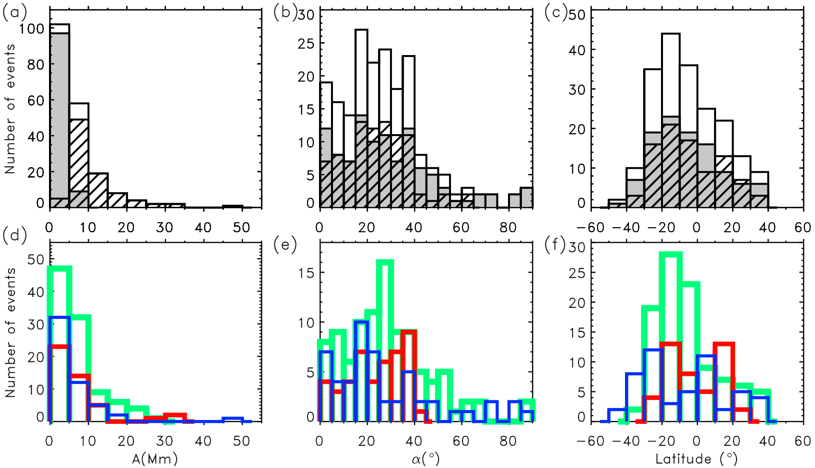

- *A* distributions for SAOs and LAOs differ.
- α distribution has a peak close to 18° and a mean value of $27^\circ \pm 18^\circ$.
- # events decreases for $\alpha > 40^\circ$ as $V - \alpha$,$|\tau/P|$-α and $A - \alpha$ scatter plots.
- Two poputions: 163 events with $\alpha < 40^\circ$ and 33 with $\alpha > 40^\circ$.
- Latitudes between 50° and -50°, typical for solar maximum.

Prominence oscillations modelling:

Transverse oscillations

- From Hyder (1966) and Kleczek & Kuperus (1969) we can obtain

$$B(G) = (5.5 \pm 3)\frac{L(\mathrm{Mm})}{P(\mathrm{min})}\,, \tag{1}$$

where we have used $n = 10^{10} - 10^{11}\mathrm{cm}^{-3}$ and the uncertainty in the numerical coefficient is associated with the uncertainty in n.

Longitudinal oscillations

- Longitudinal oscillations are driven by a combination of gravity projected along the field (pendulum model, Luna & Karpen (2012); Luna et al. (2012); Zhang et al (2012); Zhang et al. (2013)) and gas pressure gradients (slow modes, Joarder & Roberts (1992)):

$$\omega^2 = \frac{g}{R} + \omega_{\mathrm{slow}} \sim \frac{g}{R} \tag{2}$$

- The magnetic tension in the dipped part of the tubes must be larger than the weight of the threads (Luna et al. (2014)) and $n = 10^{10} - 10^{11}\mathrm{cm}^{-3}$ as the main source of uncertainty and determined that

$$B(G) \geq (0.28 \pm 0.15)\, P(\mathrm{min})\,. \tag{3}$$

Seismology in GONG catalog

- Without additional data analysis and field extrapolation, it is difficult to establish which catalog events are oscillations parallel or perpendicular to the magnetic field.
- However, our statistical analysis revealed a clear distinction between oscillations with $\alpha < 40^\circ$ and those with $\alpha > 40^\circ$.
- Although the two populations are not necessarily uniquely associated with different oscillation polarizations, for seismology purposes we applied the longitudinal model to the oscillations with $\alpha < 40^\circ$ and the transverse model to the $\alpha > 40^\circ$ cases.
- This is also justified because the two models predict approximately the same *B* for a given event.

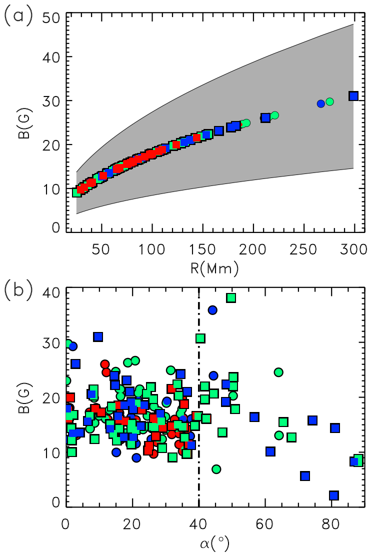

- (top panel) We determined B and R from previous equations for the events with $\alpha < 40^\circ$. The shaded area covers the uncertainties in B.
- The magnetic field ranges from 9 to 48 G, and R from 25 to 300 Mm. The mean values are $B = 16$ G and $R = 89$ Mm.
- The obtained values are consistent with the rare direct measurements of prominence magnetic fields (Mackay et al (2010)).
- (botom panel) The pendulum model is used for events with $\alpha < 40^\circ$, and transverse model for $\alpha > 40^\circ$.
- For longitudinal oscillations ($\alpha < 40^\circ$) the B range generally decreases with α, reminiscent of the behavior of P. The same trend applies to the transverse oscillations ($\alpha > 40^\circ$), although some events reach large B values (38 G).

Summary and Conclusions

- 106 SAOs ($< 10\,\mathrm{km\,s^{-1}}$) and 90 LAOs ($> 10\,\mathrm{km\,s^{-1}}$).
- Both SAOs and LAOs are common, with one event of each class every two days on the visible side of the Sun.
- For nearly half of the events, we identified their apparent trigger.
- Periods distribution mean of 58$\pm$15 min for LAOs and SAOs and filament types.
- The distribution of the damping time per period peaks at $\tau/P = 1.75$ and 1.25 for SAOs and LAOs respectively.
- LAO damping rates depend nonlinearly on the oscillation velocity.
- α centred at 27° for all filament types $\rightarrow$ field-aligned motions.
- On average $R \approx 89$ Mm and $B \approx 16$ G.
- The catalog is available to the community online (`http://goo.gl/VxkeiV`) and is intended to be expanded to cover at least 1 solar cycle.
- **Luna, Karpen, Ballester, Muglach, Terradas, Kucera & Gilbert (2018), The Astrophysical Journal Supplement Series, 236, id. 35**

We acknowledge the support from ISSI (www.issibern.ch) to teams 324 and 413 on "Large-amplitude Oscillations in Solar Prominences" and "Large-Amplitude Oscillations as a Probe of Quiescent and Erupting Solar Prominences"